academicJournals

Vol. 16(27), pp. 1490-1500, 5 July, 2017
DOI: 10.5897/AJB2017.16024
Article Number: D9090CB65018
ISSN 1684-5315

http://www.academicjournals.org/AJB

African Journal of Biotechnology

Full Length Research Paper

Silver nanoparticles biosynthesis and impregnation in cellulose acetate membrane for anti-yeast therapy

Taciana A. Silva[1], Patrícia F. Andrade[2], Karen Segala[2,3], Larissa S. C. Silva[1], Larissa P. Silva[1], Silvia V. G. Nista[4], Lucia H. I. Mei[4], Nelson Durán[2,5,6] and Maria F. S. Teixeira[1*]

[1]Parasitology Department, Federal University of Amazonas, Manaus, AM, Brazil.
[2]Chemistry Institute, University of Campinas, 13083-970, Campinas, SP, Brazil.
[3]Chemistry Department, Federal University of Amazonas, Manaus-AM, Brazil.
[4]Department of Polymer Technology, University of Campinas, 13083-970, Campinas, SP, Brazil.
[5]Brazilian Nanotechnology National Laboratory (LNNano-CNPEM), Campinas, SP, Brazil.
[6]Laboratory of Nanomaterials Synthesis and Biological Interactions (NanoBioss), Chemistry Institute, University of Campinas, Campinas, SP, Brazil.

Received 5 April, 2017; Accepted 15 June, 2017

Silver nanoparticles (AgNPs) are nanoforms that express higher antimicrobial potential due to their shape and reduced size. The use of fungi to mediate the synthesis of AgNPs has increased the interest of scientists because of their rapid growth, large-scale cultivation and secretion of non-toxic molecules. The aim of this study was to synthesize AgNPs mediated by *Aspergillus oryzae* DPUA 1624 and evaluate the antimicrobial activity of these molecules incorporated in cellulose acetate nanomembranes (NanoMAC). The synthesis of AgNPs was confirmed by UV-visible spectroscopy and the characterization was performed by dynamic light scattering, transmission electron microscopy, X-ray diffraction, X-ray dispersive energy and advanced spectroscopy and spectroscopy methods. The synthesis of the membrane was done by electro-spinning and its thickness was analyzed in scanning electron microscope. The AgNPs were added to NanoMAC and the antimicrobial effect was evaluated by agar diffusion method against *Staphylococcus aureus*, *Escherichia coli* and *Candida albicans*. The aqueous extract of *A. oryzae* mediated the synthesis of AgNPs with rounded and some triangular shapes. The diameter and zeta potential of these particles were 61.15±11.45 nm and -28.7 mv, respectively. The NanoMAC with AgNPs showed an increase in antifungal activity of 24.22% when tested against *C. albicans*. This study demonstrated that *A. oryzae* is able to mediate AgNP synthesis with anti-yeast action and the impregnation of AgNPs in acetate cellulose nanomembranes resulted in the development of a more efficient antimicrobial nanocomposite.

Key words: Silver nanoparticles, *Aspergillus oryzae*, cellulose nanofibers, anti-yeast.

INTRODUCTION

Silver nanoparticles (AgNPs) are nanoforms that express higher antimicrobial potential due to their shape and reduced size. The characters of AgNPs promote a better interaction with biological receptors, they intensify the interaction with cell surface and, consequently, they increase the bioactive efficiency (Tarafdar and Raliya, 2013; Pereira et al., 2014). Due to their excellent antimicrobial action, AgNPs are widely used in medical, technological and agricultural areas (Ingale and Chaudhari, 2013; Pereira et al., 2014; Moghaddam et al.,

2015; Siddiqi and Husen, 2016).

The world market of nanotechnological products have been in evolution. The annual arrecadation is around 25% and the prevision is an increase to 3 billions until 2020. Among these products, the ones from AgNPs stand out. The antimicrobial properties of AgNPs make possible their use in a wide diversity of products as plastics, soaps, pastes, food and textile products (Tran et al., 2013).

The colloidal solution of AgNPs can be combined with many polymeric matrices to extend the release of antimicrobial and increase its biocompatibility. The electrospinning nanofibers, for example, are polymers that have high potential of application in pharmaceutical and cosmetic industries for regeneration of skin and organs, therapies of drugs administration and others (Nista et al., 2015; Segala et al., 2015).

The search for nanostructured polymers with antimicrobial action are increasing due to their great potential of use in devices that require antiseptic characters as applications in skin wounds (Abdelgawad et al., 2013; Segala et al., 2015). For that reason, AgNPs are the nanoforms most used in polymers due to their electronic, optical, catalytic and antimicrobial properties (Segala et al., 2015).

The use of nanomembranes for the treatment of skin wounds provides better comfort to the patient because it reduces the number of antibiotic applications and doses, decreasing the side effects. In these kinds of infections, the nanomembranes also can act like a sponge absorbing all the fluids from the lesion and insure the oxygenation through the porous net of nanofibers (Nista et al., 2013).

The cellulose acetate is a polymer that presents good tenacity, high biocompatibility and relative low cost, besides, easily forms pellicles with porous structure, the characters that make it advantageous to build an antiseptic nanocomposite to wounds treatment (Nista et al., 2012; Segala et al., 2015).

The combination of AgNPs with polymers for application in many areas is very versatile. However, the method of chemical synthesis generates toxic residues that contaminate the environment and affect the ecosystem (Zhang et al., 2011; Dhanasekaran et al., 2011; Durán and Marcato, 2011; Kulkarni and Muddapur, 2014; Meva et al., 2016). In the last years, there is an increasing demand to for the development of processes mediated by microbial sources due to their low cost and the production of nontoxic molecules and for being ecofriendly (Mishra and Singh, 2015; Moghaddam et al., 2015; Siddiqi and Husen, 2016).

Among the microbial sources, the filamentous fungi are potential biologic factories to the production of metallic nanoparticles due to their fast growth, large scale cultivation, secretion of proteins with higher reducer properties and the production of molecules that stabilize nanoparticles (Durán et al., 2011; Tarafdar and Raliya, 2013; Phanjom and Ahmed, 2015).

Some species of fungi are alternative safe systems as intermediate for the AgNPs synthesis in function of their high tolerance and capacity of metallic absorption. *Aspergillus, Fusarium, Trichoderma, Cladosporium, Pleurotus, Penicillium* and *Verticillium* are examples of fungi that mediate the extracellular synthesis of AgNPs. The extracellular process is more desirable than the intracellular because is less expensive and difficult (Sastry et al., 2003; Roy et al., 2013; Siddiqi and Husen, 2016).

There are many reports in the literature showing the synthesis of AgNPs mediated by *Aspergillus* species but are rare studies showing the potential of amazonic fungi in this process. The interaction of biological AgNPs with cellulose acetate nanomembranes is also an inedited investigation because most of the researches present the development of antiseptic polymers using AgNPs obtained from chemical synthesis.

This investigation shows the capacity of *Aspergillus oryzae* DPUA 1624 to mediate AgNPs synthesis with antimicrobial potential and the anti-yeast action with the impregnation of these particles in cellulose acetate nanomembranes (NanoMAC).

MATERIALS AND METHODS

Morphological and molecular authentication of *A. oryzae*

A. oryzae DPUA 1624 (Culture Collection DPUA/UFAM) was maintained on CYA agar surface [Czapek dox agar + 0.5% (w/v) yeast extract] in plates under refrigeration (4°C) (Klich and Pitt, 1988). The macro and micro morphological identification were carried out according to Raper and Fennel (1977).

The molecular authentication was made from partial sequence of rDNA. The colony mycelium (200 mg) was used for DNA extraction by phenol chloroform method. The Internal Transcribed Spacer Region (ITS2) and part of 5.8S and 28S subunits from rDNA were amplified by PCR using ITS-3 (5´-GCA TCG ATG AAG AAC GCA GC-3') developed by White et al. (1990) and UNI-R (5'-GGT CCG TGT TTC AAG ACG-3') developed by Haynes et al. (1995). The rDNA sequences were obtained by automated sequencing (3500 ABI Applied Biosystem) and the species confirmation by comparison of DNA sequences from GeneBank using Basic Local Alignment Search Tool (BLASTn) from National Center for Biotechnology Information (NCBI).

Biomass production

A. oryzae was inoculated, by a spore suspension of 10^6 spores/ml, in 200 ml of MGYP [0.3% (w/v) malt extract; 0.1% (w/v) glucose;

*Corresponding author. E-mail: mteixeira@ufam.edu.br.

0.3% (w/v) yeast extract; and 0.5% (w/v) peptone]. Fermentation was conducted at 25°C, 180 rpm, for 96 h. The biomass was separated by filtration using Whatman paper no. 1, washed three times with ultrapure water, transferred to Erlenmayer flasks containing 200 ml of ultrapure water and maintained at 28°C, 200 rpm, for 96 h. The biomass was filtrated again and the aqueous extract recovered was used for AgNPs biosynthesis (Sastry et al., 2003; Durán et al., 2007; Vigneshwaran et al., 2007).

Silver nanoparticles biosynthesis

The aqueous extract (200 ml) was mixed with a silver nitrate solution (1 mol L^{-1}) until final concentration of 1 mmol L^{-1} and incubated at 28°C, 200 rpm for 96 h, in the absence of light. Simultaneously, two controls: one of the aqueous extract and other of nitrate solution were maintained under same conditions. The synthesis of silver nanoparticles was confirmed by the color change of the solution and the presence of plasmonic band in 400 nm (Vigneshwaran et al., 2007; Zomorodian et al., 2016). Ultraviolet-visible (UV-Vis) spectral analysis was done by using Cary 60 Agilent Spectrophotometer in the range of 200 to 800 nm.

Silver nanoparticles characterization

Zeta potential and size of AgNPs (DLS)

The AgNPs diameter, size distribution and superficial charge obtained were measured in Nano Zetasizer (ZS) (Malvern Instruments, Worcestershire, UK), at 25°C.

Transmission electron microscopy (TEM)

Size distribution and morphological variation of AgNPs were determined from high resolution images in TEM (Carl Zeiss CEM 902) operating at 80 KeV. A drop of nanoparticles solution (diluted ten times) was deposited on carbon-coated copper grid and the images were processed in *image J* software and the equation used to calculate de AgNPs diameter from the obtained area was $D = \sqrt{(\frac{A}{\pi})}$. The statistical analysis was carried out using the software origin (version 8.5.1.315).

X-Ray diffraction (XRD)

XRD patterns were performed on a Shimadzu XRD7000 with a high-power CuKα radioactive source at 40 kV/30 mA, 2° min^{-1} acanning speed, angles of 2θ from 5 to 90°.

Fourier-transform infrared spectroscopy (FTIR)

The data of IR spectra were acquired using an Agilent cary 630 FTIR spectrometer, with diamond attenuated total reflectance (ATR) attachment. In ATR mode, the spectral variation was from 400 to 4000 cm^{-1}. The AgNPs were analyzed depositing a drop of the colloidal suspension on ZnSe (zinc selenide) window.

Energy dispersive X-ray (EDX) and inductively coupled plasma optical emission spectrometry (ICP-OES)

The EDX was carried out in a Micro fluorescence x-ray spectrometer (microEDX1300, Shimadzu) in five points of the sample using spectrums of 15 and 50 kV and courting time of 200 s.

The inductively coupled plasma optical emission spectrometry (ICP-OES) was used for quantification of silver in the solution of AgNPs. The analysis was carried out in plasma emission spectrometer (PerkinElmer, Optima 8000). The calibration curve was constructed using 9 silver nitrate solutions with concentrations from 0.1 to 50 mg/L. The AgNPs solution was diluted 10 times for reading in the equipment.

Synthesis of cellulose acetate nanomembrane (NanoMAC)

The cellulose acetate (CA) polymer solution was prepared by mixing 15% (w/v) cellulose acetate into dimethylacetamida (DMAc)/Acetone (1:2). This solution was stirred for approximately 2 h to ensure its complete homogenization (Nista et al., 2012).

CA membranes were prepared by electrospinning the cellulose acetate solution at room temperature (25°C) and 50% humidity, using a 20 ml glass syringe fitted with a 4 cm long, 0.8 mm diameter metallic needle. The positive pole of a high voltage power supply was connected to the metallic needle of the syringe, while the ground electrode was used to ground the copper plate collector, which had dimensions of 30 × 40 cm. The feed stream was controlled by a KD Scientific pump, Model 100 (Campinas, Brazil) connected to a syringe. The distance from the needle to the collector was 10 cm; the applied voltage was 15 kV, and the flow rate was 1 ml h^{-1}. Membrane samples were collected in aluminium foil used to coat the copper plate during the experiments (Nista et al., 2012; Segala et al., 2015).

The morphological structure and uniformity of nanoMAC were observed in scanning electron microscope (JEOL JSM-6360LV), by vacuum, operated at 10 kV. The images were obtained after sample metallization with a layer of gold/palladium and the diameter was calculated in Image J software.

The nanoMAC coating was performed by slow dripping of the AgNPs solution in discs (5 mm) of the nanostructured membrane until the final concentration of 6.73 µg Ag on each nanoMAC disc.

Antimicrobial activity

AgNPs suspension

The agar diffusion method was used for the antimicrobial activity against *Escherichia coli* CBAM 0001, *Staphylococcus aureus* ATCC 25923 and *Candida albicans* DPUA 1706 (Ostrosky et al., 2008). The bacterial cultures (10^8 CFU/ml) were inoculated on Müller Hinton agar (MHA) and the yeast culture (10^6 CFU/ml) on Sabouraud agar (SAB) and incubated at 37°C. In each plate, 100 µl of biosynthesized AgNPs (134.5 mg/L) were transferred to wells (8 mm) made on agar surface. The plates were incubated at 37°C for 24 h. The positive controls [streptomycin (50 µg/ml) to bacteria and itraconazole (50 µg/ml) to the yeast] were maintained at the same conditions. After incubation, the plates were examined for the presence of an inhibition zone.

NanoMAC impregnated with AgNPs

The antimicrobial activity of nanoMAC impregnated with AgNPs was carried out against *C. albicans* DPUA 1706 (10^6 CFU/ml) by agar diffusion method (Ostrosky et al., 2008) in Petri dishes containing Sabouraud agar. Discs of nanoMAC (5 mm diameter) impregnated with AgNPs (6.73 µg) were compared to suspension of AgNPs (6.73 µg). The plates were incubated at 37°C for 48 h. The positive control [itraconazole (6.73 µg/ml) and itraconazole (6.73 µg/ml) + AgNPs (6.73 µg/ml)] was maintained at the same conditions.

RESULTS AND DISCUSSION

Morphological and molecular authentication of *A. oryzae*

The macro and microscopic characteristics of the culture confirmed that the fungus is *A. oryzae* (Raper and Fennel, 1977; Klick and Pitt, 1988). For the molecular authentication, the rDNA sequences presented 99% of similarity (Score, 1554) (Evalue 0) with sequences at the same region from *A. oryzae* (Access number KT964480.1). The amplified sequence of *A. oryzae* DPUA 1624 was deposited at GenBank (Access number KY655350).

Silver nanoparticles biosynthesis

The biosynthesis of silver nanoparticles (AgNPs) was confirmed by the color change of the mycelial aqueous extract from yellow to brown (Figure 1A). There was no formation of aggregate particles and the extract did not present color intensification after 96 h. These results indicate that the nanoparticles were dispersed in the solution.

The color change occurs due to the effect of superficial plasmon resonance (SPR) and the reduction of $AgNO_3$ (Li et al., 2012). SPR refers to the collective oscillation of free electrons in the metallic nanoparticles when they interact with electromagnetic radiation (Cao et al., 2011; González et al., 2014; Al Juraifani and Ghazwani, 2015).

The absorption spectrum of the AgNPs solution (Figure 1B) shows a SPR band with peak of absorbance in 446 nm confirming the presence of AgNPs after 96 h of incubation. Similar results were reported for AgNPs from *Aspergillus tubingensis* in the same wavelength (Rodrigues, 2013).

Silver nanoparticles characterization

Zeta potential and size of AgNPs

Zeta potential (ζ) indicates the repulsion between the disperse particles with the same charge by electrophoretic mobility. Its value can be related to the stability of colloidal dispersions (Phanjom and Ahmed, 2015). In this study, the zeta potential of AgNPs mediated by *A. oryzae* was 28.7 mv. This result suggests that the AgNPs have an elevated electrostatic repulsion which contributes to their stabilization. According to Roy et al. (2013), particles in suspension with high negative or positive zeta potential tend to repel themselves and do not form aggregates.

Dynamic light analysis (DLS) is a technique that determines particles sizes by measurement of aleatory changes in the intensity of light from a solution or suspension (Fatima et al., 2015). The average hydrodynamic diameter of *A. oryzae* AgNPs by DLS was 57.88 nm (Figure 2) and the polydispersity index was 0.217, confirming the formation of particles in nano scale dimension (1-100 nm) and the definition of the solution as monodisperse due to the interval defined for this type of particles from 0.01 to 0.7 (Honary et al., 2013; Tarafdar and Raliya, 2013).

Transmission eletron microscopy (TEM)

The results of TEM images (Figure 3A) show that AgNPs are predominately rounded and, in less quantity, some are triangle with average size of 61.15±11.45 nm. AgNPs with variable shapes and sizes are common in the biological systems; however, the ones with triangle shapes have more antimicrobial efficiency than the rounded AgNPs (Pal et al., 2007; Rai et al., 2009; Roy et al., 2013).

The size distribution of AgNPs is as shown in Figure 3B. Most of the AgNPs are from 50 to 60 nm in size. Some studies report nanoparticles from *Aspergillus* with sizes from 1 to 140 nm (Sagar and Ashok, 2012; Khalil, 2013; Roy and Das, 2015). Binupriya et al. (2010) and Pereira et al. (2014) reported AgNPs synthesis by *A. oryzae* species with sizes of 5 to 50 nm and 25 to 76 nm, respectively.

X-Ray diffraction (XRD)

The XRD patterns of the AgNPs showed the crystalline nature of the sample and confirmed the presence of pure silver in the nanoparticles solution analyzed. Figure 4 shows that it is possible to observe five distinct bands in 37,97°, 44,29°, 64,66°, 77,46° and 81,44° corresponding to (111), (200), (220), (311) and (222) planes. These planes correspond to the Ag° nanoparticles face-centered cubic (fcc) (Crystal Structure Database-ICSD/Code 64,994) with a lattice parameter of a = 4.077 Å. They confirm the formation of metallic silver in the suspension of AgNPs.

The absence of the bands face-centered cubic 27.9°, 32.3°, 46.3°, 55.0°, 57.6°, 67.6°, 74.6°, 76.9°, and 85.7° corresponding to the indexed (111), (200), (220), (311), (222), (400), (331), (420), and (422) facets that are typical of XRD pattern of AgCl nanoparticles (Crystal Structure Database-ICSD/Code 64734) show that there was no formation of hybrid Ag/AgCl nanoparticles as final product of the reaction (Durán et al., 2016). The unassigned peaks at 2θ = 28°, 32°, and 36° in Figure 4 are thought to be related to crystalline and amorphous organic phases (Awwad et al., 2013). These results confirm that the molecules from *A. oryzae* are efficient reducers of silver ions.

Fourier-transform infrared spectroscopy (FTIR)

The spectra presented four distinct bands: 3288, 2101, 1994 and 1633 cm^{-1} (Figure 5). The 3288 cm^{-1} band is

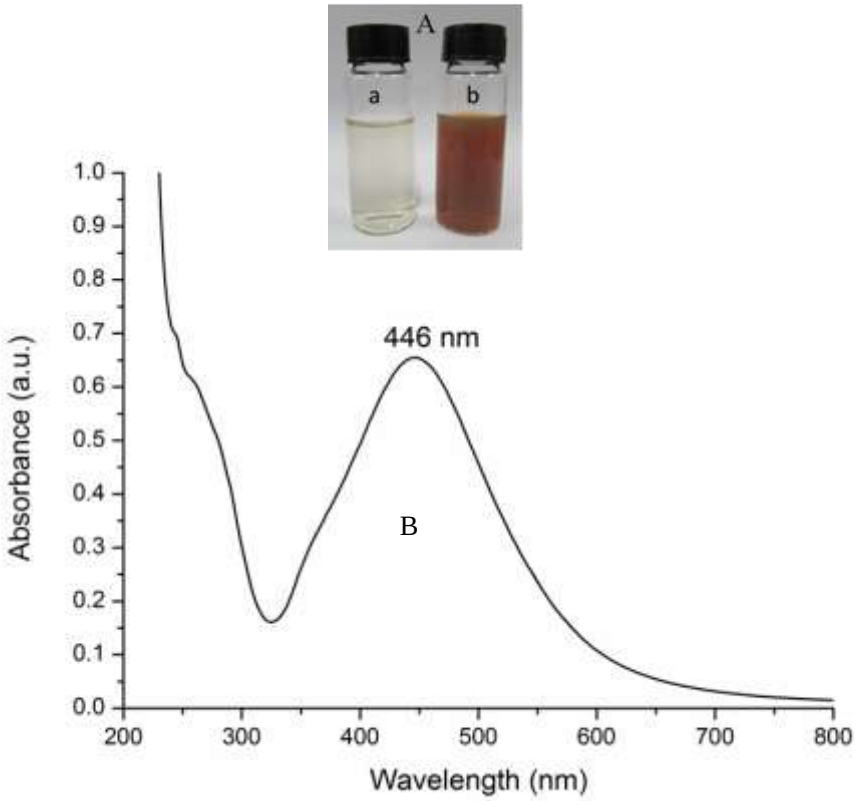

Figure 1. (A) Mycelial aqueous extract from *A. oryzae* DPUA 1624: (a) without $AgNO_3$; (b) with $AgNO_3$ (1 mol.L^{-1}); **(B)** UV-vis absorption spectrum of AgNPs after 96 h of reaction.

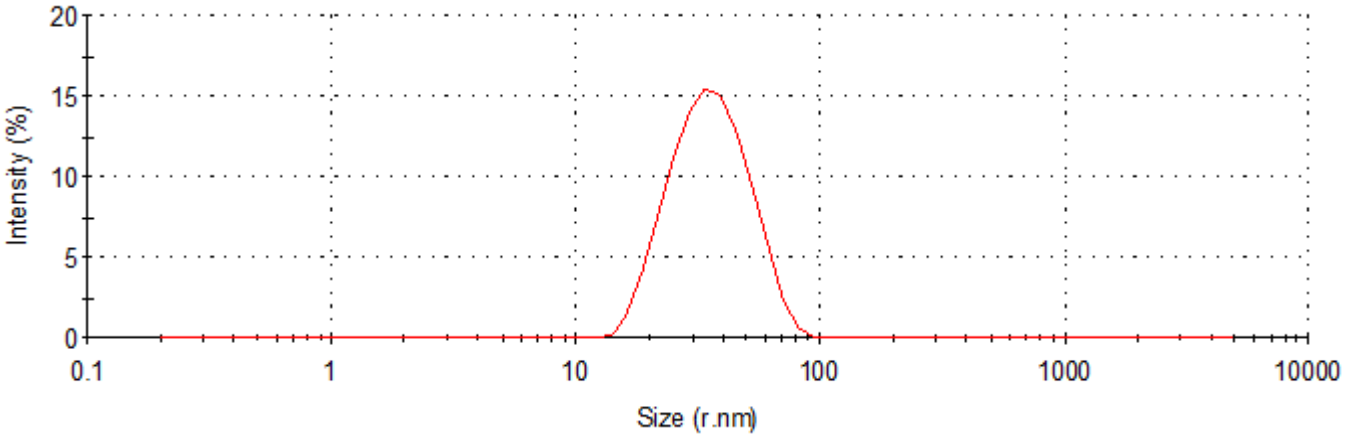

Figure 2. Hydrodinamic diameter of AgNPs biosynthetized by *A. oryzae* mycelial extract.

related to the vibration energy of primary and secondary amides from proteins and the 1633 cm^{-1} band is related to the vibration energy of carbonyl group and is assigned to the primary amide bond of the protein (El-Aziz et al., 2012). The presence of carbonyl and primary amide groups indicate that the proteins present in the aqueous extract of *A. oryzae* biomass are connected to the AgNPs. Many reports testify that proteins can connect to silver nanoparticles by the free amine groups turn them more stable particles (Phanjom and Ahmed, 2015).

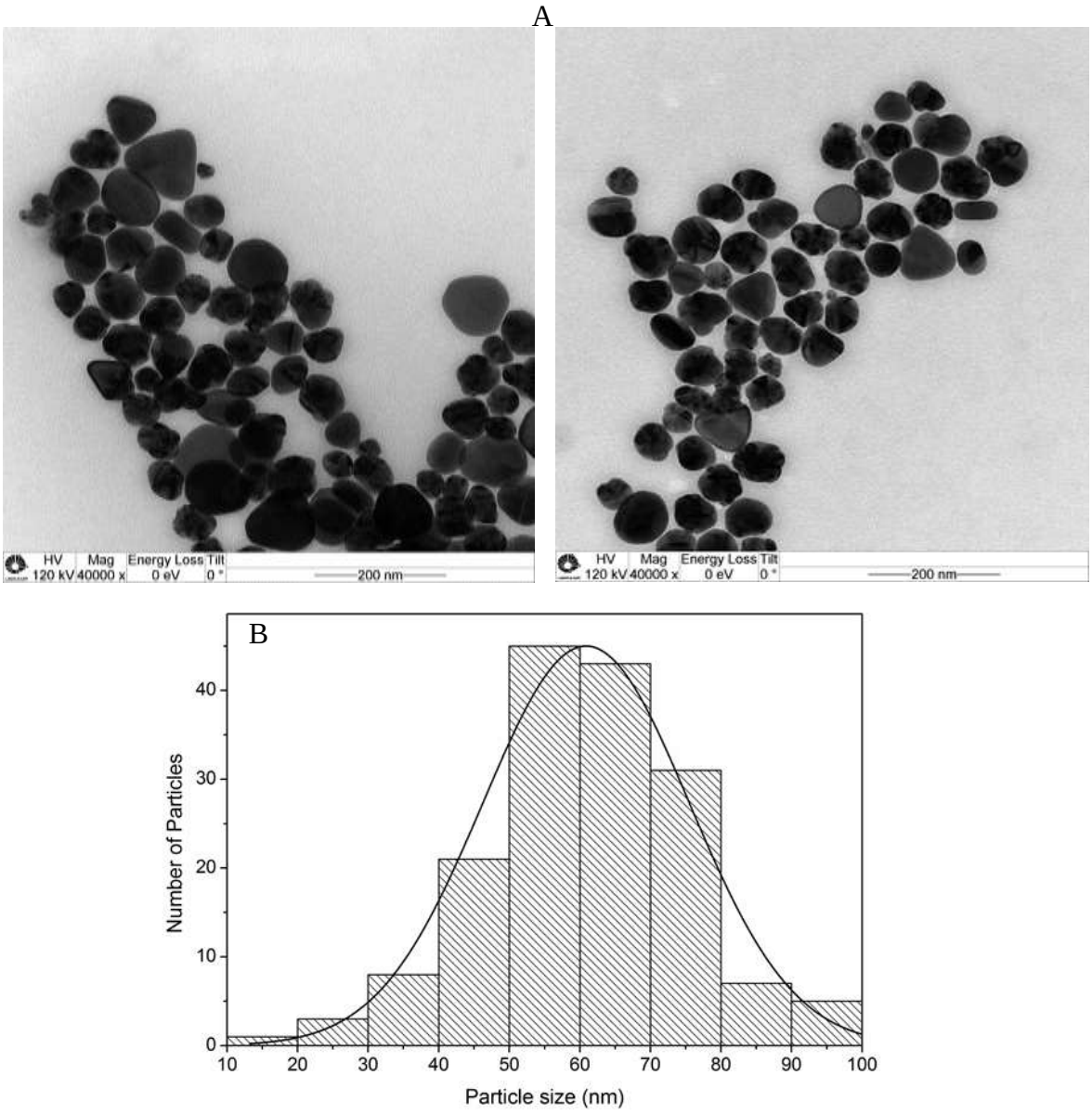

Figure 3. (A) Transmission electron microscopy images of AgNPs biosynthetized by *A. oryzae* mycelial extract. **(B)** Distribution histogram of AgNPs sizes.

Energy dispersive X-ray spectroscopy (EDX) and inductively coupled plasma optical emission spectrometry (ICP-OES)

The energy dispersive X-ray spectroscopy (EDX) revealed strong sign in the region next to 3 KeV that correspond to the peak of silver (Pereira et al., 2014; Elgorban et al., 2016). In EDX spectra, a peak was observed in 2.98 keV and others in 3.17 keV that correspond to bonds energy of AgLa and AgLb1, respectively (Figure 6). Both peaks composed of the optical absorption profile of silver element. These results indicate that the AgNP mediated by *A. oryzae* are high pure.

The inductively coupled plasma optical emission spectrometry analysis showed that the concentration of the AgNPs solution was 134.5 µg/ml.

Antimicrobial activity

AgNPs solution and NanoMAC impregnated with AgNPs

The antimicrobial activity with the AgNPs solution

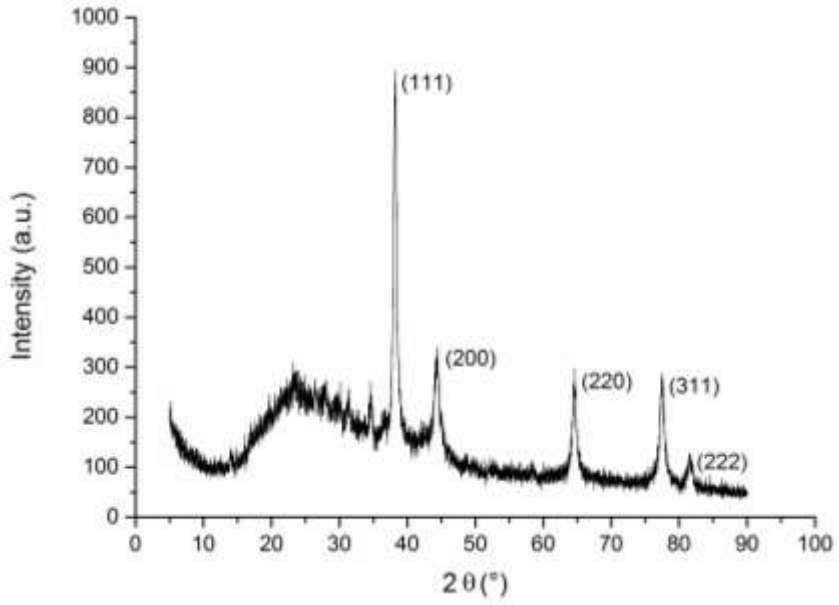

Figure 4. XRD patterns of lyophilized AgNPs biosynthetized by *A. oryzae* mycelial extract.

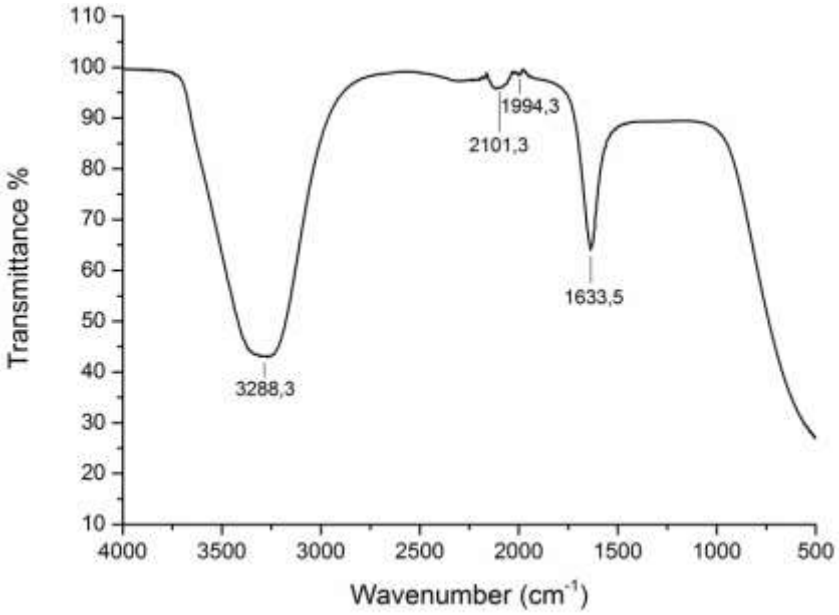

Figure 5. FTIR spectra of AgNPs biosynthetized by *A. oryzae* mycelial extract.

showed that *E. coli* CBAM 0001 and *S. aureus* ATCC 25923 were resistant to the AgNPs (134 µg/ml), while *C. albicans* DPUA 1706 was sensible. The yeast growing was completely inhibited by the AgNPs showing an inhibition zone of 23.6 cm (Figure 7).

Xue et al. (2016) reported similar results with AgNPs mediated by *Arthroderma fulvum*. The particles presented antifungal activity against many fungi including *C. albicans*.

AgNPs present efficient antimicrobial properties compared to other molecules due to their large superficial area that promotes a better contact with the micro-organims (Rai et al., 2009; Kon and Rai, 2013). However, according to Segala et al. (2015), the antimicrobial activity of AgNPs depends on some factors such as crystallinity, geometry, size, superficial oxidation,

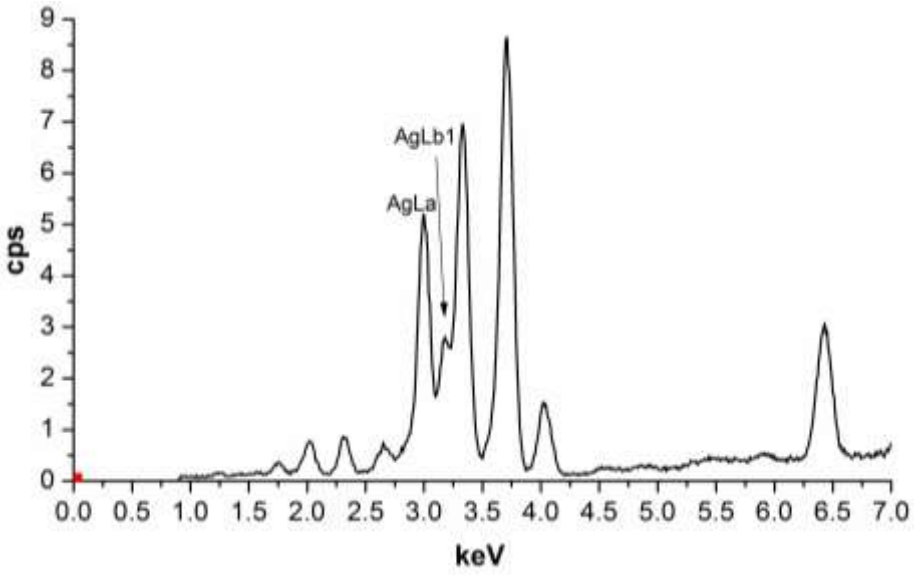

Figura 6. Energy dispersive X-ray spectra (EDX) of AgNPs solution biosynthetized by *A. oryzae* mycelial extract.

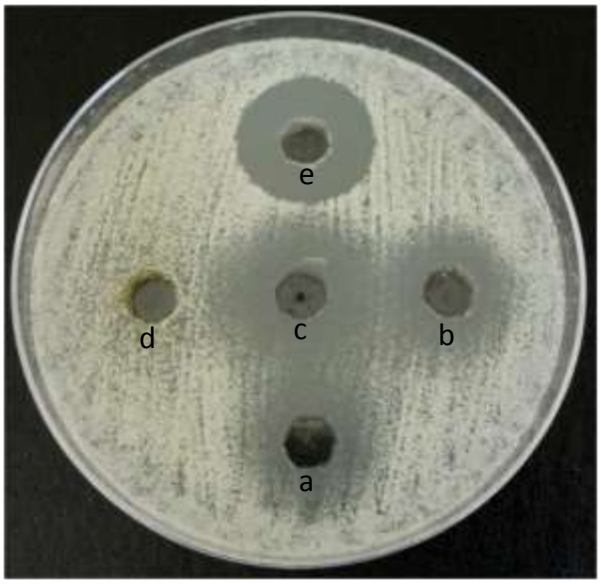

Figure 7. Antimicrobial activity of *A. oryzae* AgNPs against *C. albicans*: (a), (b) and (c) inhibitions zones formed by the AgNPs [134 µg/ml], (d) 1 mmol L^{-1} of $AgNO_3$, (e) itraconazole (50 µg/ml).

agglomeration in the biological environment, superficial charge, groups present in the nanoparticles surface, and others. For that reason, we can deduce that the properties of *A. oryzae* AgNPs enabled a better interaction with the yeast cells promoting the penetration of the nanoparticles through the plasmatic membrane of the micro-organism causing cell death.

The AgNPs antimicrobial effects are widely known, although their action mechanism in yeast cells not been completely described. Kim et al. (2009) observed that the AgNPs interact with *C. albicans* cells causing significant changes in their membranes resulting in the formation of “pits” and finally, the formation of pores and death. The authors also believe that the AgNPs break the membrane permeability barrier of *C. albicans* by the disarray of the lipid bilayer. It causes the scape of ions and other materials and the formation of pores that dissipate the membrane electrical potential.

Although many studies report the cytotoxic and genotoxic action of AgNPs in human and animal cells, there is still a lack of consistent and trustable data about them. Some of them are contradictory and, for that reason, there is no general consense about the action of these molecules in living organisms and in the environment (Rai et al., 2017). The cytotoxicity of AgNPs depends on many factors as size, shape, stability, given dose and time of exposition (Tran et al., 2013; Rai et al., 2017).

The AgNPs biosynthetized by the mycelial extract of *A. oryzae* DPUA 1624 can be evaluated as efficient agent for use in clinical application, especially in treatments of infections caused by *C. albicans.*

Yeasts highlight as main etiologic agent of fungal diseases primarily dermatomycosis, a skin infection that have been considerably increasing in the last decades. One of the causes that favor the incidence of this disease is due to the resistance of these fungi to the medications. For that reason, a considerable motivation occurs which is to find new anti-yeasts agents (Sidrim and Rocha, 2010; Xue et al., 2016).

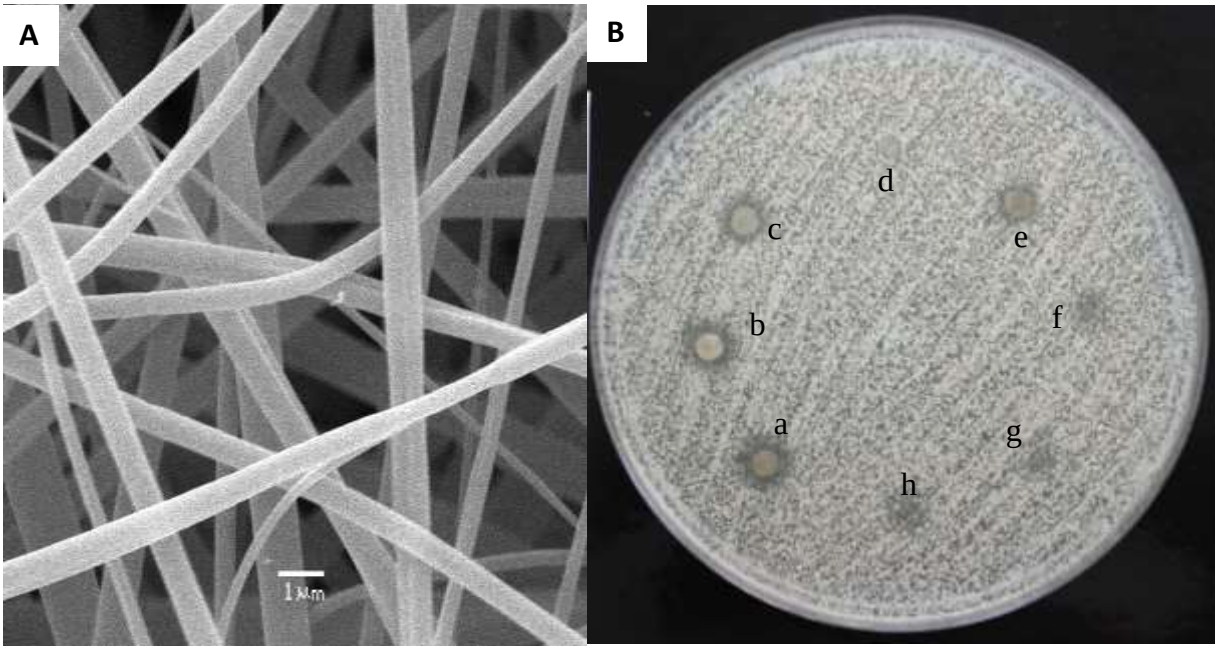

Figure 8. (A) Image in scanning electron microscope of cellulose acetate membrane (nanoMAC). **(B)** Antimicrobial activity of AgNPs impregnated in nanoMAC against *C. albicans*: (a), (b) and (c) nanofibers with AgNPs (6.73 µg); (d) nanofiber without AgNPs; (e) nanofiber with itraconazole + AgNPs (6.73 µg each); (f), (g) and (h) AgNPs 6.73 µg.

Table 1. Antimicrobial activity of AgNPs from *A. oryzae*.

Micro-organisms		Antimicrobial activity [Inhibition zone (mm)]		
		AgNPs [134 µg/ml][a]	AgNPs (6.73 µg)[a]	NanoMAC impregnated with AgNPs (6.73 µg)
Bacteria	*Escherichia coli* CBAM 0001	Resistance	na	na
	Staphylococcus aureus ATCC 25923	Resistance	na	na
Yeast	*Candida albicans* DPUA 1706	23.6±3.82	9.66±0.44	12±0.67

[a]AgNPs in colloidal solution-agar diffusion method. Na, not avaiable.

According to the necessity to develop new strategies against skin infections caused by yeasts, this study carried out the antimicrobial activity of AgNPs impregnated in cellulose acetate membrane (15%) and DMAc: acetone (1:2) (NanoMAC). The nanoMAC contains nanofibers with average diameter of 410.76 nm. They are random deposited forming a thinny and homogeneous tissue without beads formation (Figure 8A).

The nanoMAC impregnated with AgNPs (Table 1), allowed the increase of 24.22% in antifungal action against *C. albicans* when compared with the antimicrobial activity using the colloidal solution of AgNPs (Figure 8B). This result is relevant because it demonstrates that the AgNPs impregnation in cellulose acetate membrane can potentiate the action against yeasts of *Candida* genus.

NanoMAC impregnated with biological AgNPs present a large potential to be used in medical and pharmaceutical industries. They can be considered as sustainable nanocomposites with anti-yeast action.

Conclusion

The fungi *A. oryzae* DPUA 1624 produces molecules capable to reduce silver (Ag) ions and mediate stable silver nanoparticles synthesis. They are monodisperse with antimicrobial activity. This result provides a viable and eco-friendly alternative to antifungal production based on AgNPs without causing any polluting residues. The impregnation of AgNPs in cellulose acetate membrane increases the anti-yeast action of these particles resulting in the development of a nanocomposite with antifungal properties that can be used in medical and pharmaceutical industries.

CONFLICT OF INTERESTS

The authors have not declared any conflict of interests.

ACKNOWLEDGEMENTS

The authors thank the scientific support of workers and students from the laboratories of Biologic Chemistry, Analytical Center of the Chemistry Institute, Biomaterials of Chemical Engineer College of Campinas University (UNICAMP), Laboratory of Nanomaterials Synthesis and Biological Interactions (NanoBioss), Brazilian Nanotechnology National Laboratory (LNNano-CNPEM), Instituto Nacional de C,T&I em Materiais Complexos Funcionais (INOMAT-MCTI/CNPq) and Culture Collection DPUA of Federal University of Amazonas (UFAM). They also thank the financial support from Rede de Biodiversidade e Biotecnologia da Amazônia Legal (BIONORTE), Conselho Nacional de Desenvolvimento Científico e Tecnológico (CNPq/CT-Amazônia) and Fundação de Apoio à Pesquisa do Estado de São Paulo (FAPESP).

REFERENCES

Abdelgawad AM, Hudson SM, Rojas OJ (2013). Antimicrobial wound dressing nanofiber mats from multicomponent (chitosan/silver-NPs/polyvinyl alcohol) systems. Carbohydr. Polym. 100:166-178.

Al Juraifani AAA, Ghazwani AA (2015). Biosynthesis of silver nanoparticles by *Aspergillus niger*, *Fusarium oxysporum* and *Alternaria solani*. Afr. J Biotechnol. 14(26):2170-2174.

Awwad AM, Salem NM, Abdeen AO (2013). Green synthesis of silver nanoparticles using carob leaf extract and its antibacterial activity. Int. J. Ind. Chem. 4(1):29.

Binupriya AR, Sathishkumar M, Yun SI (2010). Myco-crystallization of silver ions to nanosized particles by live and dead cell filtrates of *Aspergillus oryzae* var. wiridis and its its bacterial activity toward *Staphylococcus aureus* KCCM 12256. Ind. Eng. Chem. Res. 49:852-858.

Cao W, Huang T, Xu X-HN, Elsayed-Ali HE (2011). Localized surface plasmon resonance of single silver nanoparticles studied by dark-field optical microscopy and spectroscopy. J. Appl. Phys. 109(34310):1-6.

Dhanasekaran D, Latha S, Saha S, Thajuddin N, Panneerselvam A (2011). Biosynthesis and antimicrobial potential of metal nanoparticles. Int. J. Green Nanotechnol. Biomed. 3(1):72-82.

Durán N, Marcato PD (2011). Biotechnological routes to nanoantimicrobials and industrial: mechanistics aspects, antimicrobial activity, toxicity and industrial implications. In. Rai M, Cioffi N, editors. Nano-Antimicrobials: Progress and Prospects. Germany: Springer. In Press.

Durán N, Marcato PD, Durán M, Yadav A, Gade A, Rai M (2011). Mechanistic aspects in the biogenic synthesis of extracellular metal nanoparticles by peptides, bacteria, fungi, and plants. Appl. Microbiol. Biotechnol. 90(5):1609-1624.

Durán N, Marcato PD, Souza GIH, Alves OL, Esposito E (2007). Antibacterial effect of silver nanoparticles produced by fungal process on textile fabrics and their effluent treatment. J. Biomed. Nanotechnol. 3(2):203-208.

Durán N, Nakazato G, Seabra AB (2016). Antimicrobial activity of biogenic silver nanoparticles, and silver chloride nanoparticles: an overview and comments. Appl. Microbiol. Biotechnol. 100(15):6555-6570.

El-Aziz ARMA, Al-Othman MR, Alsohaibani SA, Mahmoud MA, Sayed SRM (2012). Extracellular biosynthesis and characterization of silver nanoparticles using *Aspergillus niger* isolated from Saudi Arabia (strain KSU-12). Dig. J. Nanomater. Biostruct. 7(4):1491-1499.

Elgorban AM, El-Samawaty AE, Yassin MA, Sayed SR, Adil SF, Elhindi KM, Bakri M, Khan M (2016). Antifungal silver nanoparticles: synthesis, characterization and biological evaluation. Biotechnol. Biotechnol. Equip. 30(1):56-62.

Fatima F, Bajpai P, Pathak N, Singh S, Priya S, Verma SR (2015). Antimicrobial and immunomodulatory efficacy of extracellularly synthesized silver and gold nanoparticles by a novel phosphate solubilizing fungus *Bipolaris tetramera*. BMC Microbiol. 15(52):1-10.

González AL, Noguez C, Beránek J, Barnard AS (2014). Size, shape, stability, and color of plasmonic silver nanoparticles. J. Phys. Chem. C. 118(17):9128-9136.

Haynes KA, Westerneng TJ, Fell JW, Moens W (1995). Rapid detection and identification of pathogenic fungi by polymerase chain reaction amplification of large subunit ribosomal DNA. J. Med. Vet. Mycol. 33:319-325.

Honary S, Barabadi H, Gharaei-fathabad E, Naghibi F (2013). Green Synthesis of Silver Nanoparticles Induced by the Fungus *Penicillium citrinum*. Trop. J. Pharm. Res. 12(1):7-11.

Ingale AG, Chaudahari AN (2013). Biogenic synthesis of nanoparticles and potential applications: an eco- friendly approach. J. Nanomed. Nanotechnol. 4(2):10-17.

Kulkarni N, Muddapur U (2014). Biosynthesis of Metal Nanoparticles. J. Nanotechnol. 2014:1-8.

Khalil NM (2013). Biogenic silver nanoparticles by *Aspergillus terreus* as a powerful nanoweapon against *Aspergillus fumigatus*. Afr. J. Microbiol. Res. 7(50):5645-5651.

Kim KJ, Sung WS, Suh BK, Moon SK, Choi JS, Kim JG, Lee DG (2009). Antifungal activity and mode of action of silver nano-particles on *Candida albicans*. Biometals 22(2):235-242.

Klich MA, Pitt JI (1988). A Laboratory guide to common *Aspergillus* species and their teleomorphs. Australia: North Ryde, N.S.W.: Commonwealth Scientific and Industrial Research Organisation, Division of Food Processing. 116p.

Kon K, Rai M (2013). Metallic nanoparticles: mechanism of antibacterial action and influencing factors. J. Comp. Clin. Pathol. Res. 2(1):160-174.

Li G, He D, Qian Y, Guan B, Gao S, Cui Y, et al (2012). Fungus-mediated green synthesis of silver nanoparticles using *Aspergillus terreus*. Int J Mol Sci. 13(1):466-476.

Meva FE, Segnou ML, Ebongue CO, Ntoumba AA, Steve DY, Malolo FA, Ngah L, Massai H, Mpondo EM (2016). Unexplored vegetal green synthesis of silver nanoparticles: A preliminary study with *Corchorus olitorus* Linn and *Ipomea batatas* (L.) Lam. Afr. J. Biotechnol. 15(10):341-349.

Mishra S, Singh HB (2015). Biosynthesized silver nanoparticles as a nanoweapon against phytopathogens: exploring their scope and potential in agriculture. Appl. Microbiol. Biotechnol. 99(3):1097-1107.

Moghaddam AB, Namvar F, Moniri M, Tahir PM, Azizi S, Mohamad R (2015). Nanoparticles biosynthesized by fungi and yeast: A review of their preparation, properties, and medical applications. Molecules 20(9):16540-16565.

Nista SVG, Bettini J, Lucia Helena Innocentini Mei (2015). Coaxial Nanofibers of Chitosan-Alginate-PEO polycomplex 2 obtained by electrospinning. Carbohydr. Polym. 127:222-228.

Nista SVG, D'Avila MA, Martinez EF, Silva A de SF, Mei LHI (2013). Nanostructured membranes based on cellulose acetate obtained by electrospinning, Part II: Controlled release profile and microbiological behavior. J. Appl. Polym. Sci. 2:2772-2779.

Nista SVG, Peres L, D'Avila MA, Schmidt FL (2012). Nanostructured membranes based on cellulose acetate obtained by electrospinning, Part 1: study of the best solvents and conditions by design of experiments. J. Appl. Polym. Sci. 126:E70-E78.

Ostrosky EA, Mizumoto MK, Lima MEL, Kaneko TM, Nishikawa SO, Freitas BR (2008). Methods for evaluation of antimicrobial activity and determination of minimum inhibitory concentration (MIC) of medicinal plants. Braz. J. Pharmacogn. 18(2):301-3077.

Pal S, Tak YK, Song JM (2007). Does the antibacterial activity of silver nanoparticles depend on the shape of the nanoparticle? A study of the gram-negative bacterium *Escherichia coli*. Appl. Environ. Microbiol. 73(6):1712-1720.

Pereira L, Dias N, Carvalho J, Fernandes S, Santos C, Lima N (2014). Synthesis, characterization and antifungal activity of chemically and fungal-produced silver nanoparticles against *Trichophyton rubrum*. J. Appl. Microbiol. 117:1601-1613.

Phanjom P, Ahmed G (2015). Biosynthesis of Silver Nanoparticles by *Aspergillus oryzae* (MTCC No . 1846) and Its Characterizations. Nanosci Nanotechnol. 5(1):14-21.

Rai M, Ingle AP, Paralikar P, Gupta I, Medici S, Santos CA (2017). Recent advances in use of silver nanoparticles as antimalarial agents. Int. J. Pharm. 526(1-2):254-270.

Rai M, Yadav A, Gade A (2009). Silver nanoparticles as a new generation of antimicrobials. Biotechnol. Adv. 27(1):76-83.

Raper KB, Fennell DI (1977). The Genus *Aspergillus*. New York, N.Y: Robert E. Krieger Co, 686p.

Rodrigues AG (2013). Application of mangrove fungi to obtain antimicrobial silver nanoparticles. Dissertation (Master in Biotechnology) - Institute of Biomedical Sciences, University of São Paulo, São Paulo. 106p.

Roy S, Das TK (2015). A review on biosynthesis of silver nanoparticles using *Aspergillus* species. Adv. Sci. Eng. Med. 7(9):729-738.

Roy S, Rukherjee T, Chakraborty S, Das TK (2013). Biosynthesis, characterisation & antifungal activity of silver nanoparticles synthesized by the fungus *Aspergillus foetidus* MTCC8876. Dig. J. Nanomater. Biostruct. 8(1):197-205.

Sagar G, Ashok B (2012). Green synthesis of silver nanoparticles using A*spergillus niger* and its efficacy against human pathogens. Eur. J. Exp. Biol. 2(5):1654-1658.

Sastry M, Ahmad A, Islam Khan M, Kumar R (2003). Biosynthesis of metal nanoparticles using fungi and actinomycete. Curr. Sci. 85(2):162-170.

Segala K, Nista SV, Cordi L, Bizarria MT, Ávila Júnior JD, Kleinubing SA, Cruz DC, Brocchi M, Lona LM, Caballero NE, Mei LH (2015). Silver nanoparticles incorporated into nanostructured biopolymer membranes produced by electrospinning : a study of antimicrobial activity. Braz. J. Pharm. Sci. 51(4):911-921.

Siddiqi KS, Husen A (2016). Fabrication of metal nanoparticles from fungi and metal salts: scope and application. Nanoscale Res. Lett. 11(98):1-15.

Sidrim JJ, Rocha MFG (2010). Medical Mycology in the Light of Contemporary Authors. Rio de Janeiro: Guanabara Koogan; 388p.

Tarafdar JC, Raliya R (2013). Rapid, low-cost, and ecofriendly approach for iron nanoparticle synthesis using *Aspergillus oryzae* TFR9. J. Nanoparticles 2013:1-4.

Tran QH, Nguyen VQ, Le A-T (2013). Silver nanoparticles: synthesis, properties, toxicology, applications and perspectives. Adv. Nat. Sci. Nanosci. Nanotechnol. 4(3):33001.

Vigneshwaran N, Ashtaputre NM, Varadarajan PV, Nachane RP, Paralikar KM, Balasubramanya RH (2007). Biological synthesis of silver nanoparticles using the fungus *Aspergillus flavus*. Mater. Lett. 61(6):1413-1418.

White T J, Bruns T, Lee S TJW (1990). Amplification and direct sequencing of fungal ribosomal RNA genes for phylogenetics. In. Innis MA, Gelfand D H, Sninsky JJWTJ, editor. PCR protocols: a guide to methods and applications. New York, N.Y: Academic Press, Inc. Pp. 315-322.

Xue B, He D, Gao S, Wang D, Yokoyama K, Wang L (2016). Biosynthesis of silver nanoparticles by the fungus *Arthroderma fulvum* and its antifungal activity against genera of *Candida*, *Aspergillus* and *Fusarium*. Int. J. Nanomed. 11:1899-1906.

Zhang X, Yan S, Tyagi RD, Surampalli RY (2011). Synthesis of nanoparticles by microorganisms and their application in enhancing microbiological reaction rates. Chemosphere 82(4):489-494.

Zomorodian K, Pourshahid S, Sadatsharifi A, Mehryar P, Pakshir K, Rahimi MJ, Arabi Monfared A (2016). Biosynthesis and characterization of silver nanoparticles by *Aspergillus* species. BioMed. Res. Int. pp. 1-6.